



Missouri University of Science and Technology  
Scholars' Mine

---

Electrical and Computer Engineering Faculty  
Research & Creative Works

Electrical and Computer Engineering

---

01 Mar 2010

## Novel and Simple High-Frequency Single-Port Vector Network Analyzer

Mohamed A. Abou-Khousa

Mark A. Baumgartner

Sergey Kharkovsky

*Missouri University of Science and Technology*

R. Zoughi

*Missouri University of Science and Technology, zoughi@mst.edu*

Follow this and additional works at: [https://scholarsmine.mst.edu/ele\\_comeng\\_facwork](https://scholarsmine.mst.edu/ele_comeng_facwork)

 Part of the [Electrical and Computer Engineering Commons](#)

---

### Recommended Citation

M. A. Abou-Khousa et al., "Novel and Simple High-Frequency Single-Port Vector Network Analyzer," *IEEE Transactions on Instrumentation and Measurement*, vol. 59, no. 3, pp. 534-542, Institute of Electrical and Electronics Engineers (IEEE), Mar 2010.

The definitive version is available at <https://doi.org/10.1109/TIM.2009.2024701>

This Article - Journal is brought to you for free and open access by Scholars' Mine. It has been accepted for inclusion in Electrical and Computer Engineering Faculty Research & Creative Works by an authorized administrator of Scholars' Mine. This work is protected by U. S. Copyright Law. Unauthorized use including reproduction for redistribution requires the permission of the copyright holder. For more information, please contact [scholarsmine@mst.edu](mailto:scholarsmine@mst.edu).

# Novel and Simple High-Frequency Single-Port Vector Network Analyzer

Mohamed A. Abou-Khousa, *Student Member, IEEE*, Mark A. Baumgartner, Sergey Kharkovsky, *Senior Member, IEEE*, and Reza Zoughi, *Fellow, IEEE*

**Abstract**—Portable, accurate, and relatively inexpensive high-frequency vector network analyzers (VNAs) have great utility for a wide range of applications, encompassing microwave circuit characterization, reflectometry, imaging, material characterization, and nondestructive testing to name a few. To meet the rising demand for VNAs possessing the aforementioned attributes, we present a novel and simple VNA design based on a standing-wave probing device and an electronically controllable phase shifter. The phase shifter is inserted between a device under test (DUT) and a standing-wave probing device. The complex reflection coefficient of the DUT is then obtained from multiple standing-wave voltage measurements taken for several different values of the phase shift. The proposed VNA design eliminates the need for expensive heterodyne detection schemes required for tuned-receiver-based VNA designs. Compared with previously developed VNAs that operate based on performing multiple power measurements, the proposed VNA utilizes a single power detector without the need for multiport hybrid couplers. In this paper, the efficacy of the proposed VNA is demonstrated via numerical simulations and experimental measurements. For this purpose, measurements of various DUTs obtained using an X-band (8.2–12.4 GHz) prototype VNA are presented and compared with results obtained using an Agilent HP8510C VNA. The results show that the proposed VNA provides highly accurate vector measurements with typical errors on the order of 0.02 and 1° for magnitude and phase, respectively.

**Index Terms**—Phase shifter, power detector, reflection coefficient, standing-wave probe, vector network analyzer (VNA).

## I. INTRODUCTION

HIGH-PERFORMANCE vector network analyzers (VNAs) are the most prominent measurement instruments used to characterize circuits and devices at radio, microwave, millimeter-wave, and submillimeter-wave frequencies [1], [2]. The VNA is designed to measure vector scattering parameters, i.e., the complex reflection coefficient, of a device under test (DUT) connected at its test port, without disturbing the waves at that port. Therefore, the actual signal measurements within the VNA are typically performed at another location or port, and subsequently, the vector parameter

at the test port is inferred or calculated from these measurements [3].

In general, VNAs can be realized based on coherent and noncoherent detection schemes. A VNA with coherent detection scheme measures the in-phase and quadrature components of the complex signal reflected at or transmitted through the test port. This is accomplished by utilizing a tuned receiver, e.g., a heterodyne receiver architecture [4]. Nowadays, commercial VNAs operating based on this detection scheme are the most developed instruments for high-frequency vector measurements. Since the tuned receiver detection scheme is inherently narrow band in nature, e.g., a narrow-band intermediate frequency stage, these VNAs usually offer a large measurement dynamic range and a very low noise floor [4]. However, the high complexity and cost associated with implementing the tuned receiver, i.e., the need for highly stable phase-locked sources, limits the utility of such VNAs in many applications where simple, handled, and relatively inexpensive high-frequency *in situ* vector-measuring devices are needed.

On the other hand, automatic VNA systems based on noncoherent detection offer a relatively inexpensive and simple alternative to the tuned receiver VNAs. With noncoherent detection, the complex signal magnitude and phase are inferred from simple power measurements. Multiprobe [5], six-port [3], [6], and multistate [7] reflectometers are among the pioneering designs upon which VNA designs based on noncoherent detection schemes were realized. The measurement dynamic range of these systems is limited by the relatively low dynamic range of a power detector, which, for these purposes, is commonly a diode detector. However, this range can be extended using phase modulation and a locked-in amplifier [8]. Many automatic VNA systems based on these reflectometers have been proposed and successfully implemented in the past, with a recent system described in [9]. All of the aforementioned designs are fundamentally based on utilizing multiple power detectors connected to multiport junctions, i.e., hybrid couplers, which necessitates multistep characterization and calibration procedures [10].

A simple noncoherent detection-based VNA design using a single power detector and a set of perturbation-two-port (PTP) networks was proposed in [11]. The PTP approach is based on using a set of perturbation networks inserted between a DUT and a scalar network analyzer. The complex reflection coefficient of the DUT is calculated from the magnitude of the reflection coefficient measured by the scalar network analyzer using a given set of PTP networks [11].

In this paper, we introduce a novel and simple noncoherent detection-based VNA, which utilizes a single power detector

Manuscript received March 13, 2009; revised May 26, 2009. First published October 20, 2009; current version published February 10, 2010. This work was supported by the U.S. Air Force under Contract FA8103-07-C-0193. The Associate Editor coordinating the review process for this paper was Dr. Matteo Pastorino.

The authors are with the Applied Microwave Nondestructive Testing Laboratory (*amntl*), Electrical and Computer Engineering Department, Missouri University of Science and Technology, Rolla, MO 65409 USA (e-mail: maamc2@mst.edu; mabwf4@mst.edu; sergiy@mst.edu; zoughir@mst.edu).

Color versions of one or more of the figures in this paper are available online at <http://ieeexplore.ieee.org>.

Digital Object Identifier 10.1109/TIM.2009.2024701

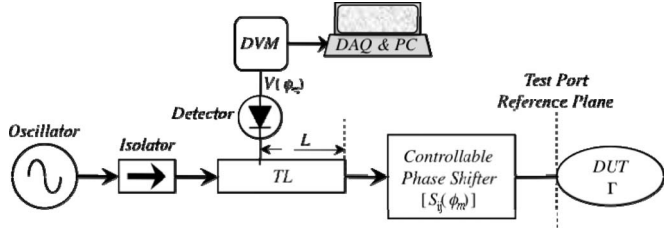


Fig. 1. Schematic of the proposed VNA.

and an electronically controllable phase shifter inserted between a DUT and a standing-wave probing device. Subsequently, the magnitude and phase of the reflection coefficient of the DUT  $\Gamma$  are uniquely determined from standing-wave voltages measured at three or more phase-shift settings. Given that the phase-shifter characteristics at these settings are known, the proposed VNA can fully be calibrated with only three standard loads, i.e., known reflections. The phase shifter can be characterized by measuring its scattering parameters either using an independent VNA or using this same VNA in conjunction with a characterization procedure involving a set of known standards.

Unlike the PTP approach, the proposed VNA design does not require a scalar network analyzer. Using a single power detector and avoiding the use of a scalar network analyzer and multiport hybrid junctions by performing standing-wave measurements are the main unique aspects of the proposed VNA, which significantly reduces its complexity compared with the previously proposed noncoherent detection-based VNAs. Given the current advanced state of small electronically controllable phase-shifter designs, implementing the proposed novel VNA design yields an accurate, wideband, robust, handheld, relatively inexpensive, and high-performance measurement device that may be used for a variety of diverse applications.

This paper describes the design of the proposed VNA and demonstrates its accuracy for complex reflection coefficient measurements. Subsequently, the VNA performance is investigated via simulations considering various critically important system parameters such as the number of phase-shift settings, relative phase shifts, characteristics of the phase shifter, and detector noise. Moreover, the experimental attributes of an X-band (8.2–12.4 GHz) prototype system is presented based on a commercially available off-the-shelf electronic phase shifter. The measurement accuracy associated with the prototype VNA is then compared with that of an Agilent HP8510C VNA.

## II. PROPOSED VNA DESIGN

The developed VNA is formed by inserting an electronically controllable phase shifter between a simple standing-wave probing device and a DUT, as shown in Fig. 1. The standing-wave probing device consists of a transmission line (TL), e.g., a straight waveguide section, with a probe attached to a diode detector. The reflected signal from the DUT is then combined with the incident signal (from the isolated oscillator) to form a standing wave in the TL. Subsequently, a diode detector located a distance  $L$  along the TL produces a dc voltage proportional to

the standing-wave power at that location. In this configuration, the phase shifter is used to electronically “move” the standing-wave pattern with respect to the detector location and hence obtain the pertinent reflection information without the need to move the detector itself, as in the slotted line method [1], or use multiple detectors along the TL, as in some realizations of six-port reflectometers [5], [12], [13].

### A. System Concept

Assuming that the diode detector is biased in the square-law region, the measured standing-wave voltage as a function of the phase shift introduced by the phase shifter is modeled by

$$V(\phi_m) = C |1 + S(\phi_m)e^{-j\beta L}|^2 \quad (1)$$

where  $C$  is a constant proportional to the incident power and the diode detector characteristics,  $\beta = 2\pi/\lambda_g$  and  $\lambda_g$  are the propagation constant and the wavelength in the TL, respectively, and

$$S(\phi_m) = S_{11}(\phi_m) + \frac{S_{21}(\phi_m)S_{12}(\phi_m)\Gamma}{1 - S_{22}(\phi_m)\Gamma} \quad (2)$$

is the effective reflection coefficient referenced to the output port of the TL after accounting for the scattering characteristics (S-parameters) of the phase shifter, i.e.,  $S_{ij}(\phi_m)$ ,  $\{i = 1, 2; j = 1, 2\}$ .

The S-parameters of the phase shifter are assumed to be known either from a system characterization procedure or from prior independent measurements using a VNA. The latter option is particularly appealing with stable phase shifters since the measured S-parameters can be saved and later used during system operation. Similarly, the propagation constant  $\beta$ , the detector location along the line  $L$ , and the constant  $C$  are assumed to be known from system characterization. Hence, the only remaining unknown in (1) is the sought-after DUT reflection coefficient  $\Gamma$ . Several phase shifts  $\{\phi_m : m = 1, 2, \dots, M\}$  and their corresponding measured standing-wave voltages  $\{V(\phi_m) : m = 1, 2, \dots, M\}$  are used to formulate a system of  $M$  nonlinear equations, which can subsequently be solved, i.e., using the Gauss–Newton method, to determine  $\Gamma$ . For example, Fig. 2 shows the actual (simulated) and calculated complex DUT reflection coefficients obtained using the proposed procedure for  $L = \lambda_g/4$ ,  $C = -1$ ,<sup>1</sup> with an ideal phase shifter, i.e.,  $S_{11}(\phi_m) = S_{22}(\phi_m) = 0$ ,  $S_{21}(\phi_m) = S_{12}(\phi_m) = e^{-j\phi_m}$ , and three phase shifts of  $\{\phi_1 = 0, \phi_2 = 10^\circ, \phi_3 = 20^\circ\}$ . As shown in Fig. 2, the obtained solution for  $\Gamma$ , which is based on using the three standing-wave voltages produced by the three phase shifts, very closely matches the actual DUT reflection used for the simulation.

For system design, it is important to find the minimum number of phase shifts  $M$  required to uniquely calculate the complex reflection coefficient of the DUT from the  $M$  voltage measurements in (1). Assuming that the discrete phase shifts

<sup>1</sup>Negative diode detector polarity is assumed throughout this paper.

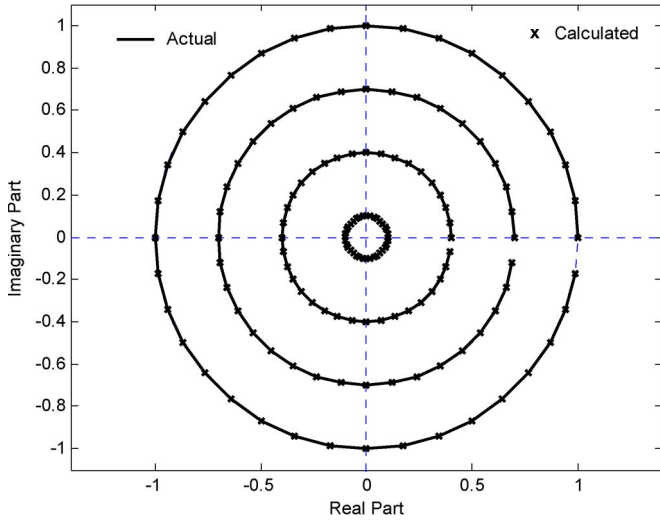


Fig. 2. Actual and calculated DUT reflection coefficients based on noise-free standing-wave voltages and three phase shifts.

are a means to sample the standing-wave pattern along the line, the minimum number of phase shifts required to accurately recover the standing-wave pattern from its samples, and consequently the reflection information, is essentially dictated by the sampling theorem. The standing-wave pattern is periodic with a period equal to half of the wavelength in the TL, i.e.,  $\lambda g/2$ . If we were to sample the standing-wave pattern using the phase shifter and a single detector, the minimum number of samples (phase shifts) is determined by the Nyquist rate. Accordingly, the minimum sampling rate required to reconstruct the standing-wave pattern of period  $\lambda g/2$  should be greater than  $4/\lambda g$ . This results in at least four samples for every  $\lambda g$  along the TL. Since the distance  $\lambda g$  in the TL corresponds to a total phase shift of  $2\pi$  rad, the sampling rate should be greater than  $2/\pi$ . Assuming that the relative phase shift interval of  $\pi$  rad ( $V(\phi_m)$  is periodic with a period of  $\pi$ ), the minimum number of required phase shifts is given by

$$M > 2 \rightarrow M_{\min} = 3. \quad (3)$$

This result is analogous to the requirement of using at least three power detectors spaced along the  $\lambda g/2$  line to insure proper sampling of the standing wave in multiprobe TL methods [5], [13].

### B. Calibration

In practice, the obtained DUT complex reflection coefficient after solving the nonlinear equations involving the phase-shifter characteristics and the corresponding standing-wave measurements might not be accurate due to various imperfections in the measurement system, i.e., reflections due to connector mismatch, losses in the TL, etc. [These were not accounted for in the model given in (1).] The effects of such imperfect hardware can collectively be modeled as systematic errors, which, in turn, can be calibrated out from the measured DUT reflection coefficient, hence enhancing the measurement accuracy.

To reduce the effects of systematic errors, the proposed VNA can be calibrated using the conventional three-term calibration procedure used with traditional four-port reflectometers [14]. Following this procedure, a fictitious error adapter representing three systemic errors is inserted between the test port and the phase shifter. The three error parameters are determined from the measured effective complex reflection coefficient of three standard (known) loads. For this purpose, termination, short, and offset short loads are used as the standard or calibration loads. The effective complex reflection coefficient, which is measured at the output port of the TL, for each standard load connected at the test port is found after solving the set of nonlinear equations involving the phase shifts and the corresponding standing-wave voltages. Subsequently, the measured DUT reflection coefficient is corrected based on the obtained error terms [14].

### C. Features

With three phase shifts, the resulting system of nonlinear equations is in fact overdetermined since the complex reflection coefficient represents only two unknowns (real and imaginary parts of  $\Gamma$ ). Hence, these equations can also simultaneously be solved to obtain  $C$ . Additional phase shifts may also be used to solve for other unknowns if needed, e.g., detector location, and, more importantly, increase the measurement accuracy through coherent averaging using many phase shifts produced via simple electronic control. Consequently, the effects of the unreliable standing-wave pattern measurements near standing-wave nulls and detector noise can significantly be reduced.

Unlike the multiprobe techniques, which are bandwidth limited due to the fixed relative placement of the detectors, the proposed design does not impose any restriction, neither on the placement of the detector nor on the values of the phase shifts for wideband coherent reflectometry measurements.

In general, the performance of the proposed VNA depends on the following factors:

- 1) detector noise level;
- 2) phase-shift interspacing;
- 3) number of phase shifts;
- 4) DUT reflection coefficient, i.e., low and high reflection coefficients;
- 5) quality of the phase shifter, i.e., return and insertion losses;
- 6) detector characteristics;
- 7) repeatability in producing phase shifts.

The effect of the first five factors will further be examined in the next section. The effect of the detector characteristics will not be addressed in this paper. The detector is assumed to produce a dc voltage proportional to the standing-wave power, i.e., operating in the square-law region. Deviations from this norm can usually be corrected using known methods [15]. The phase-shift settings should be repeatable to obtain consistent measurements. To this end, the used phase-shifter characteristics should remain constant over the course of the measurements. Phase shifters with highly repeatable phase-shift settings are very common nowadays.

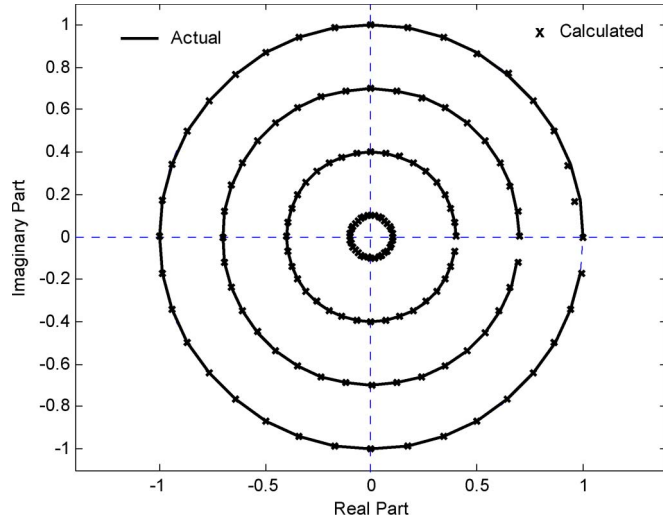


Fig. 3. Actual and calculated DUT reflection coefficients based on noisy standing-wave voltages and three phase shifts (noise RMS of 1 mV).

### III. SIMULATION RESULTS

The capability of the proposed VNA to accurately measure various DUT reflection coefficients in the presence of measurement noise, i.e., detector noise, was investigated via simulations. A VNA system with  $L = \lambda_g/4$  and  $C = -1$  was considered to illustrate the operation of the proposed VNA without the error adapter. The effect of detector noise was simulated by adding independent identically distributed noise terms to the  $M$  voltages computed from the standing-wave model as per (1) before calculating the DUT reflection coefficient  $\Gamma$ . The noise terms were modeled as samples of the Gaussian random process with zero mean and standard deviation  $\sigma$ , representing the detector noise root-mean-square (RMS) value. Fig. 3 shows the actual and calculated DUT reflection coefficients  $\Gamma$  with an ideal phase shifter producing three phase shifts of  $\{\phi_1 = 0, \phi_2 = 10^\circ, \phi_3 = 20^\circ\}$ , based on noisy standing-wave voltages ( $\sigma = 1$  mV). As shown in Fig. 3 and when compared with the noiseless results shown in Fig. 2, it is clear that the DUT reflection coefficient was uniquely determined, even in the presence of detector noise. Average performance metrics, i.e., the RMS error (RMSE), will be used next to quantify the errors introduced due to noise.

Theoretically speaking, the interspacing between the phase shifts can be arbitrarily small, and yet, an accurate estimate of the DUT reflection coefficient may still be obtained. However, due to the noise contaminating the detected voltage, the spacing between the phase shifts, within a relative phase shift interval of  $\pi$ , affects the accuracy of the measurement results. Extensive simulations were performed to study the effect of phase-shift interspacing and noise RMS on the accuracy of the obtained DUT reflection coefficient. For instance, consider measuring a DUT reflection coefficient of  $\Gamma_{\text{actual}} = 0.5e^{j\pi/4}$  using the proposed system with  $M = 3$  equally spaced phase shifts in the interval from 0 to  $\pi$ . The phase shifts were  $\{\phi_1 = 0, \phi_2 = \delta\phi, \phi_3 = 2\delta\phi\}$ , where  $\delta\phi$  is the phase-shift interspacing (in degrees) such that  $\delta\phi < 90^\circ$ . Several noise RMS values and phase-shift interspacing were considered, and the magnitude and phase average RMSEs relative to the actual (simulated)

DUT reflection coefficient were computed for combinations of noise RMS value and phase-shift interspacing. The RMSEs for magnitude and phase are defined, respectively, as

$$\text{Magnitude RMSE} = \sqrt{\frac{1}{N} \sum_{i=1}^N (|\Gamma_i| - |\Gamma_{\text{actual}}|)^2} \quad (4)$$

$$\text{Phase RMSE} = \sqrt{\frac{1}{N} \sum_{i=1}^N (\text{Angle}(\Gamma_i/\Gamma_{\text{actual}}))^2} \quad (5)$$

where  $\Gamma_i$  is the computed DUT reflection coefficient at the  $i$ th simulation run. A total of  $N = 10000$  simulation runs with different noise realizations were used to estimate the average magnitude and phase RMSEs. The RMSE is used here as a *figure-of-merit* to quantify the uncertainty in phase and magnitude measurements due to the detector noise only. The analysis of other typical sources of measurement uncertainties such as connection repeatability and calibration standards accuracy is beyond the scope of this paper.

Fig. 4(a) and (b) shows the RMSEs for magnitude and phase, respectively, as a function of the phase-shift interspacing for different noise RMS values using an ideal phase shifter with  $M = 3$ . The results show that magnitude and phase RMSE values of less than 0.01 and  $1^\circ$ , respectively, at  $\delta\phi = 10^\circ$  can be achieved with a noise RMS value as high as 10 mV. For  $\delta\phi < 10^\circ$ , the RMSEs for magnitude and phase rapidly and monotonically decrease as the phase-shift interspacing decreases for all noise levels. A marginal decrease in the RMSE performance is observed after increasing the phase-shift interspacing beyond  $\delta\phi = 10^\circ$  (the RMSE performance remains within the order of the magnitude attained at  $\delta\phi = 10^\circ$ ). It is also apparent that the RMSE performance linearly degrades as a function of increasing noise RMS value.

As the minimum number of discrete phase shifts was earlier established, it becomes important to study the improvement in the performance of the system when more than three phase shifts are used to calculate the DUT reflection coefficient. Fig. 5(a) and (b) shows the RMSEs for magnitude and phase, respectively, as a function of the number of phase shifts for different noise levels with  $\delta\phi = 10^\circ$  for the same system parameters and DUT that were earlier used. For all noise levels, increasing the number of phase shifts results in decreasing the RMSEs for both magnitude and phase. An increase beyond eight phase shifts only marginally improves the performance. The linear relationship between the noise RMS value and the RMSEs for magnitude and phase is also manifested in these results.

Since the probed standing-wave voltage dynamic range changes as a function the magnitude of the DUT reflection coefficient  $|\Gamma|$ , the accuracy of the computed reflection coefficient is also dependent on  $|\Gamma|$ . Typical magnitude RMSEs, for three phase shifts and  $\delta\phi = 10^\circ$ , as a function of  $|\Gamma|$  for different noise RMS values are shown in Fig. 6(a). The RMSE curves shown in Fig. 6(a) were normalized to the actual magnitude of the DUT reflection coefficient (directly related to the percentage error). The normalized RMSE is relatively high

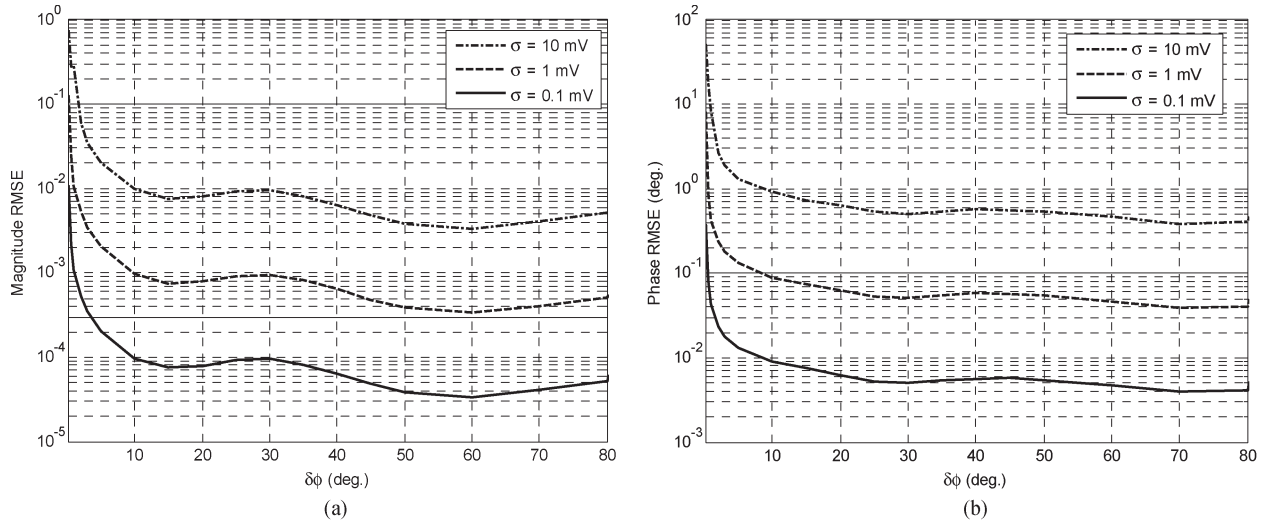


Fig. 4. (a) Magnitude and (b) phase RMSEs as obtained using the proposed VNA with  $M = 3$  as a function of the phase-shift interspacing for different noise RMS values.

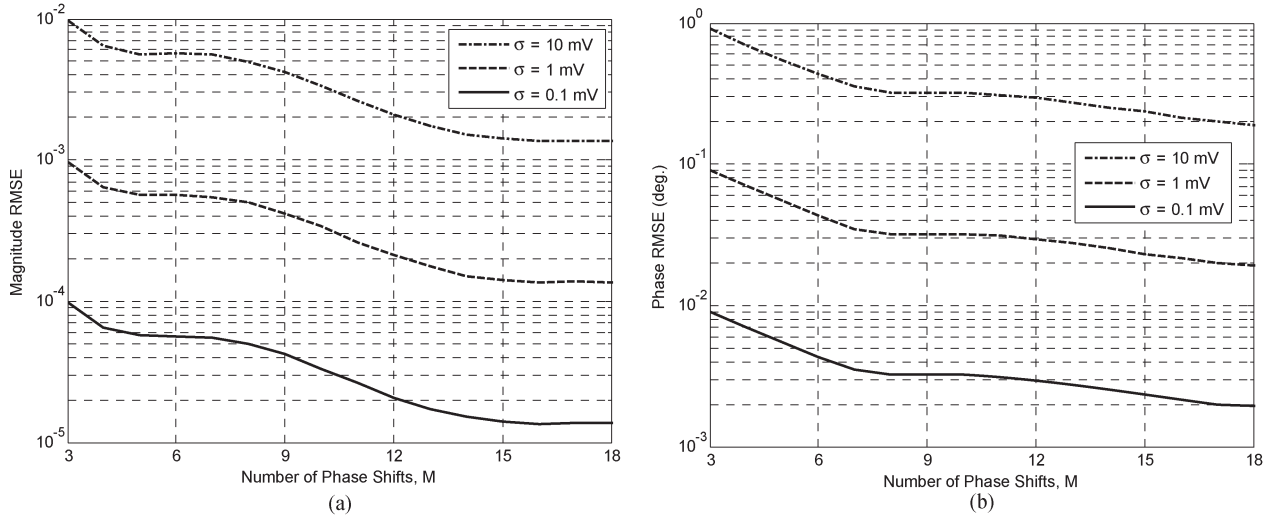


Fig. 5. (a) Magnitude and (b) phase RMSEs as obtained using the proposed VNA as a function of the number of phase shifts for different noise RMS values ( $\delta\phi = 10^\circ$ ).

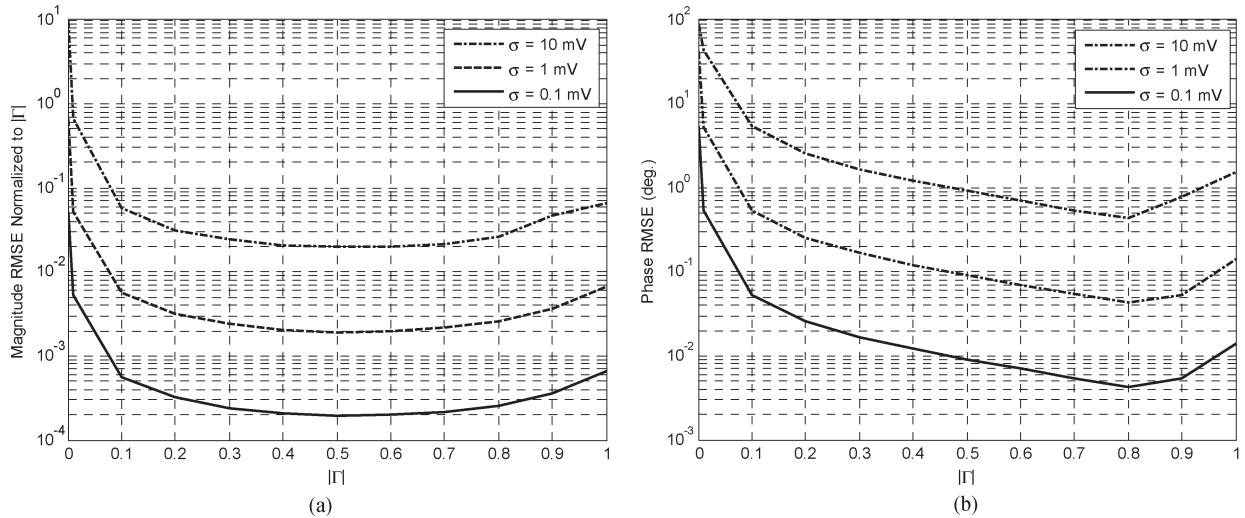


Fig. 6. (a) Normalized magnitude and (b) phase RMSEs as obtained using the proposed VNA as a function of the magnitude of the reflection coefficient ( $M = 3$  and  $\delta\phi = 10^\circ$ ).

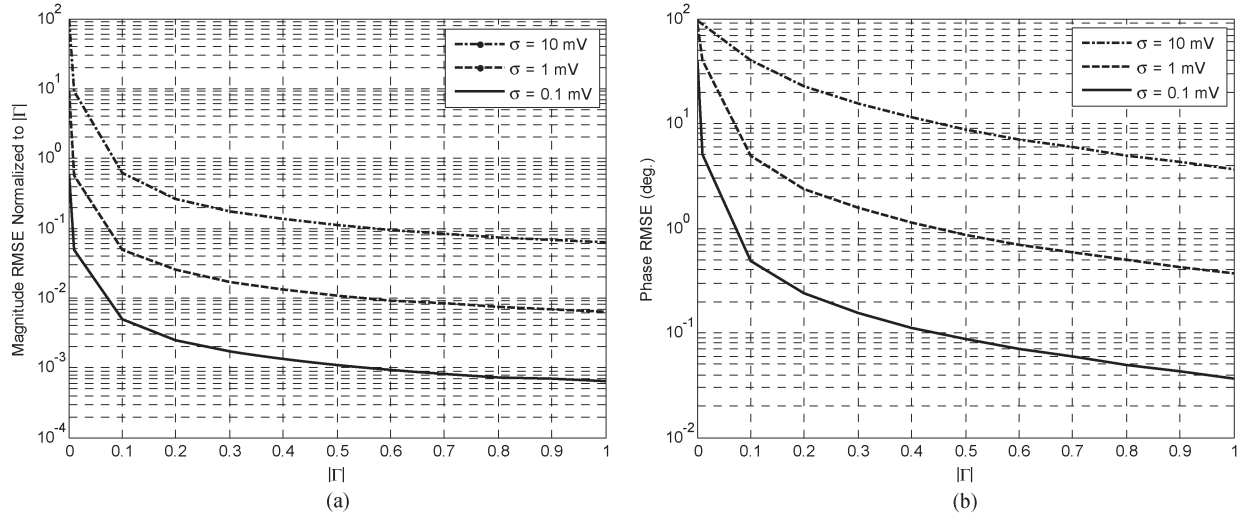


Fig. 7. (a) Normalized magnitude and (b) phase RMSEs as obtained using the proposed VNA with a nonideal phase shifter as a function of the magnitude of the reflection coefficient ( $M = 3$  and  $\delta\phi = 10^\circ$ ).

for low DUT reflections. For such low reflections, the standing-wave pattern is almost flat, and consequently, the anticipated changes in the standing-wave voltage as a function of the phase shifts can easily be masked by system noise. On the other hand, high DUT reflections cause sharp nulls in the standing-wave pattern. Reliable detection of changes in the standing-wave voltage around these nulls in the presence of noise is always problematic. Relatively better performance is obtained for the middle reflection values between these two extremes, as expected. For  $0.1 < |\Gamma| < 0.8$ , the phase RMSE is almost linear as a function of  $|\Gamma|$ , as shown in Fig. 6(b).

Thus far, the analyses and the corresponding results were for an ideal phase shifter. However, nonideal phase-shifter characteristics such as the input port return loss ( $RL_i$ ), the insertion loss (IL), and the output port return loss ( $RL_o$ ) also alter the standing-wave pattern and consequently influence the performance of the proposed VNA. To highlight this effect, the performance of the proposed VNA when using a nonideal phase shifter characterized by  $RL_i = 10$  dB,  $IL = 8$  dB, and  $RL_o = 20$  dB ( $M = 3$  and  $\delta\phi = 10^\circ$ ) was simulated. These values were chosen since they closely match the corresponding midband values of an X-band phase shifter used to construct the prototype VNA, as will be described in the next section. Fig. 7(a) and (b) shows the magnitude normalized RMSE and the phase RMSE, respectively, as a function of  $|\Gamma|$ . The high insertion loss of the phase shifter reduces the standing-wave voltage dynamic range, and hence, the accuracy with the nonideal phase shifter is, in general, lower compared with that when an ideal phase shifter is considered (see Fig. 6), as expected. The effect of standing-wave nulls on the accuracy of determining high DUT reflections is also reduced in this case since the insertion loss in the phase shifter significantly reduces these nulls. Consequently, the RMSE monotonically decreases as a function of increasing  $|\Gamma|$ .

Collectively, the simulation results show that the detector noise and the characteristics of the phase shifter have a profound effect on the performance of the proposed VNA and therefore must properly be accounted for. The uncertainties in

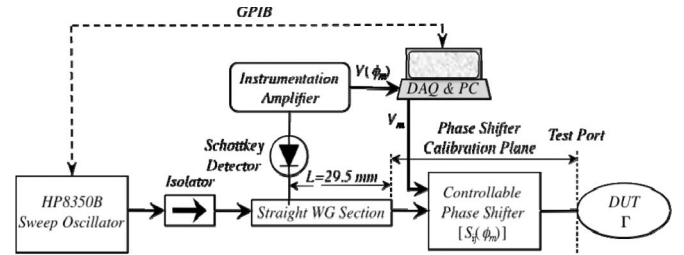


Fig. 8. Schematic of the X-band VNA prototype.

measuring the magnitude and phase of the DUT reflection coefficient linearly change with increasing noise RMS value. Hence, it becomes imperative to use low-noise power detectors and acquisition systems to obtain accurate measurement results. Coherent averaging using multiple sets of phase shifts can be implemented to reduce the combined effect of noise and reduction in the voltage dynamic range due to the losses in the phase shifter, as it will be shown later in this paper.

#### IV. MEASUREMENT RESULTS

An X-band (8.2–12.4 GHz) automated VNA prototype, as depicted in Fig. 8, was constructed and tested. The standing-wave device consisted of a straight section of an X-band rectangular waveguide and a zero-biased Schottky diode detector. The output power of the sweep oscillator was set such that the diode detector operated in the square-law region for all frequencies within the band. Since the corresponding detector output voltage is low in that region, a low-noise instrumentation amplifier was used to amplify the output voltage. A commercially available electronic phase shifter (controllable by a variable dc input voltage) was used in this implementation. The S-parameters of the phase shifter (in between the calibration planes shown in Fig. 8) were measured over the X-band using an Agilent HP8510C VNA and subsequently incorporated in the calculation of  $\Gamma$ , as per (2).

The phase-shifter input return loss, output return loss, and insertion loss are around 10 dB, 20 dB, and 8 dB, respectively,

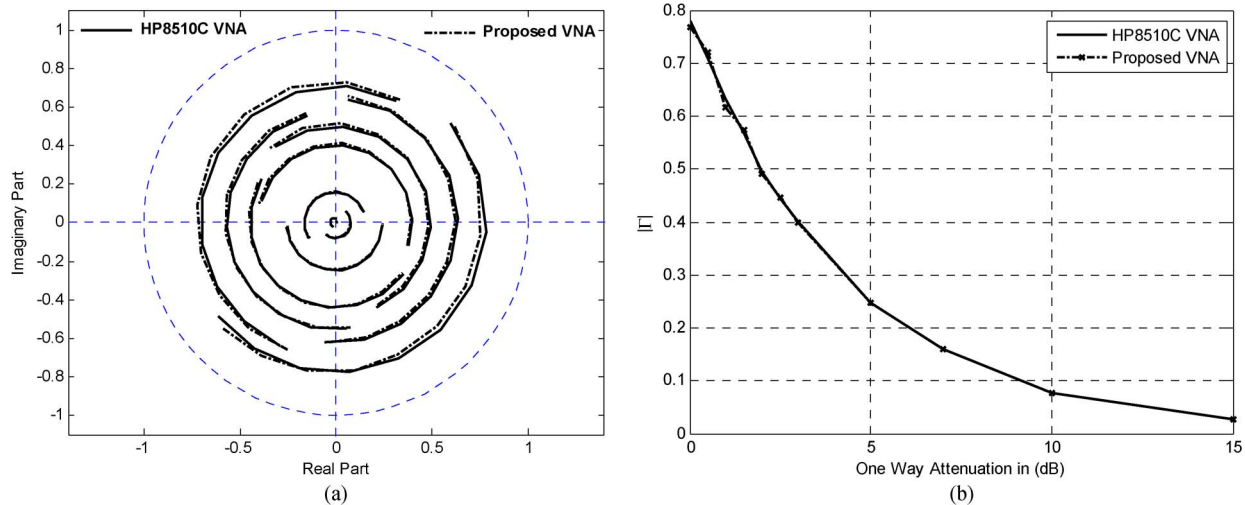


Fig. 9. Measured DUT reflection coefficient using the HP8510C VNA and the proposed VNA. (a) Real and imaginary parts of  $\Gamma$ . (b)  $|\Gamma|$  as a function of the DUT one-way attenuation.

at the center frequency of 10.3 GHz. The phase shifter provides relative phase shifts of around  $140^\circ$  and  $90^\circ$  at the beginning and toward the end of the band, respectively, in response to control voltages  $V_m$ , ranging from 0.4 to 1.2 V. Voltage steps of 0.1 V were used to control the phase shifter in that range, i.e., a total of nine discrete phase shifts. Each 0.1 V results in phase shifts of  $\sim 18^\circ$  and  $\sim 10^\circ$  at the beginning and toward the end of the band, respectively.

The system was calibrated using a short, a 0.902-cm offset short, and a matched load as calibration standards. In solving for the error terms, the standards were assumed to be ideal, and they were also used to calibrate the Agilent HP8510C VNA for comparison purposes. To account for any source and/or amplifier drifts during the course of the measurements, the constant  $C$  was simultaneously computed with the complex reflection coefficient during the measurement of the calibration standards and the DUT. Automation of the swept measurements was accomplished through a PC with a fast data acquisition (DAQ) card and a general-purpose interface bus control link. The detection system noise RMS value was estimated to be around 4 mV.

Fig. 9(a) and (b) shows the measured complex reflection coefficient of a variable DUT using the HP8510C and the proposed VNA at a frequency of 10.3 GHz. The variable DUT, which consisted of a variable phase shifter and an attenuator, terminated with a short, allowing the synthesis of various complex reflection coefficients with  $0.028 < |\Gamma| < 0.78$  ( $-2$  to  $-31$  dB) and a wide range of phase values. While all HP8510C measurements were conducted with an internal averaging factor of 16, i.e., averaging internal system noise only, the proposed VNA measurements were the results of coherent averaging of four different sets of phase shifts, each consisting of  $M = 3$  phase shifts. As shown in Fig. 9(a) and (b), the results of measurements obtained using the proposed VNA are in excellent agreement with their counterparts obtained using the HP8510C VNA. Referenced to the HP8510C VNA measurements, the average magnitude error in the proposed VNA measurements ranged from a minimum of  $7.68 \times 10^{-4}$

(for  $|\Gamma| = 0.028$ , 2.77% error) to a maximum of 0.018 (for  $|\Gamma| = 0.708$ , 2.52% error). On the other hand, the average phase errors in the ranges  $0.69^\circ$  (for  $|\Gamma| = 0.401$ ) and  $2.54^\circ$  (for  $|\Gamma| = 0.708$ ) were observed, respectively. Most of the magnitude and phase average errors are actually within the measurement uncertainties of the HP8510C VNA [16].

It is important to note that the utilized electronic phase-shifter quality is far from ideal, i.e., it presents a high insertion loss, resulting in a two-way attenuation of  $\sim 16$  dB. Nevertheless, the high measurement accuracy demonstrated with this phase shifter is attributed to the capability of performing coherent averaging of the complex reflection coefficient measurements obtained using different and multiple sets of phase shifts. This effect was also studied by performing measurements with different sets of phase shifts, each with  $M = 3$  phase shifts for the same DUT earlier described. Fig. 10 shows the RMSEs for the phase and magnitude of the measured complex reflection coefficient using the proposed VNA with one set of phase shifts and averaging the results of two, three, and four different sets. The RMSE values were computed with respect to the HP8510C VNA measurements, i.e., the HP8510C VNA measurements were used as  $\Gamma_{\text{actual}}$  in (4) and (5). As shown in Fig. 10, using one set of phase shifts did not yield accurate phase and magnitude results. However, coherent averaging of the measurements obtained using two sets of phase shifts significantly enhances the performance. Marginal improvement was obtained by averaging the results of three and four sets of phase shifts. With four sets of phase shifts, the maximum magnitude RMSE (normalized to  $|\Gamma|$ ) was  $\sim 0.03$  (for  $|\Gamma| = 0.028$ ), and a maximum phase RMSE of  $2.83^\circ$  was obtained (for  $|\Gamma| = 0.708$ ), as shown in Fig. 10.

The proposed VNA was used to perform swept frequency measurements of an arbitrary unknown DUT, and the results were compared with those obtained with the HP8510C VNA. Fig. 11 shows the magnitude and phase of the DUT complex reflection coefficient measurements over the entire X-band frequencies. The proposed VNA results were the average of the measurements obtained with four sets of phase shifts. As



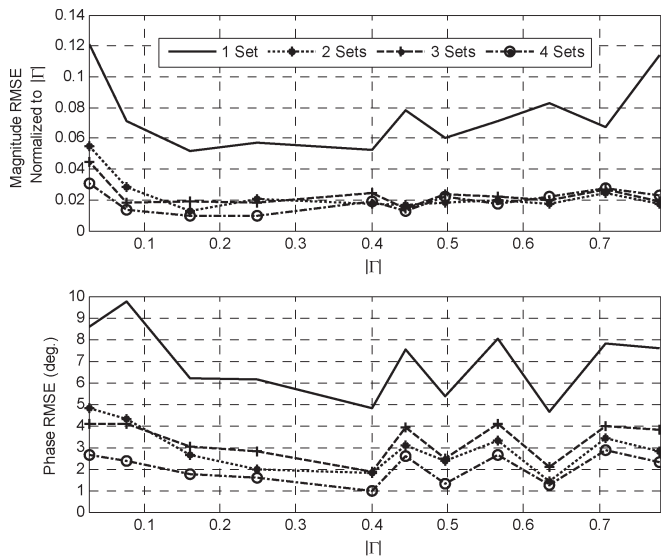


Fig. 10. (Top) Magnitude RMSE normalized to  $|\Gamma|$  and (bottom) phase RMSE as a function of  $|\Gamma|$  with averaging over different numbers of phase sets ( $M = 3$ ).

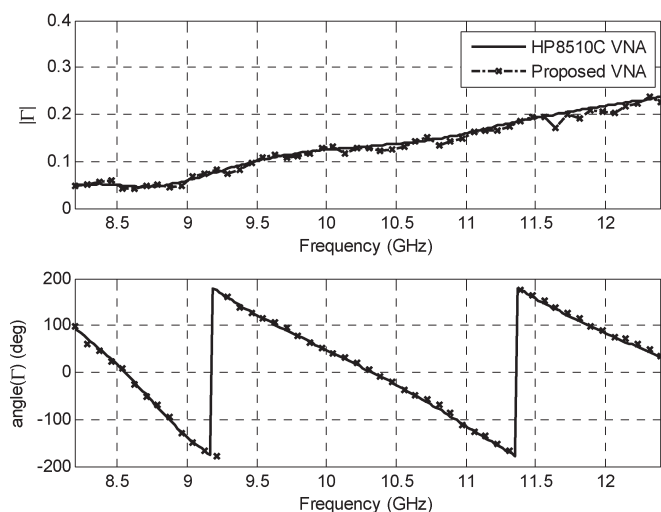


Fig. 11. (Top) Magnitude and (bottom) phase measurements of an X-band DUT obtained using the HP8510C VNA and the proposed VNA.

indicated in Fig. 11, the proposed VNA measurements closely match those of the HP8510C VNA. The proposed VNA results presented in Fig. 11 are raw measurement results corresponding to 51 frequency points in the band without any smoothing.

The proposed VNA produced highly consistent and repeatable complex reflection coefficient measurements as observed from repeatedly testing the system over long periods of time with different calibration runs. The sensitivity of the proposed VNA to changes in the phase-shifter characteristics was investigated as well. Repeated measurements of the phase-shifter characteristics showed that they remain fairly constant over time (almost 18 months), and consequently, the performance of the proposed VNA remains robust. In fact, the used phase shifter was characterized five months before taking the measurements presented in this paper. Finally, it is emphasized that higher measurement accuracy can potentially be obtained with the

proposed VNA design when a phase shifter of a higher quality, i.e., a smaller insertion loss, is used.

V. SUMMARY

Simple, handheld, relatively inexpensive, and automated VNAs are in demand for a wide range of applications requiring *in situ* vector measurements, such as microwave and millimeter-wave circuit characterization, imaging, material characterization, and nondestructive testing. For these and similar emerging applications, a novel VNA design has been introduced in this paper. The simplicity of the proposed VNA design stems from the fact that it is based on standing-wave measurements performed using a single power detector. Additionally, the proposed VNA can be calibrated following a simple procedure using only three calibration standards. The complex reflection coefficient of the DUT is inferred from three phase-shifted standing-wave measurements. An electronic phase shifter inserted between the DUT and the standing-wave probing device is controlled to yield the required phase shifts. Various attributes of the proposed design were investigated in simulations, considering the phase-shifter characteristics and the detector noise. It was shown that the uncertainties in phase and magnitude measurements linearly increase with the detector RMS value.

To demonstrate the feasibility and accuracy of the proposed VNA, an off-the-shelf electronic phase shifter was used in constructing a prototype automated X-band VNA. The prototype was used to perform swept and single-frequency measurements of various DUTs. An excellent agreement between the measurements obtained using the proposed VNA prototype and the HP8510C VNA was observed. The measurement accuracy of the proposed VNA can further be improved by utilizing a higher quality phase shifter.

REFERENCES

- [1] D. M. Pozar, *Microwave Engineering*, 2nd ed. New York: Wiley, 1998.
- [2] A. Fung, D. Dawson, L. Samoska, K. Lee, T. Gaier, P. Kangaslahti, C. Oleson, A. Denning, Y. Lau, and G. Boll, "Two-port vector network analyzer measurements in the 218–344- and 356–500-GHz frequency bands," *IEEE Trans. Microw. Theory Tech.*, vol. 54, no. 12, pp. 4507–4512, Dec. 2006.
- [3] G. F. Engen, "The six-port reflectometer: An alternative network analyzer," *IEEE Trans. Microw. Theory Tech.*, vol. MTT-25, no. 12, pp. 1075–1080, Dec. 1977.
- [4] Agilent Technologies, Inc., *Agilent AN 1287-2, Exploring the Architectures of Network Analyzers*. Application Note. [Online]. Available: <http://cp.literature.agilent.com/litweb/pdf/5965-7708E.pdf>
- [5] R. Caldecott, "The generalized multi-probe reflectometer and its application to automated transmission line measurements," *IEEE Trans. Antennas Propag.*, vol. AP-21, no. 4, pp. 550–554, Jul. 1973.
- [6] C. A. Hoer, "The six-port coupler: A new approach to measuring voltage, current, power, impedance, and phase," *IEEE Trans. Instrum. Meas.*, vol. IM-21, no. 4, pp. 466–470, Nov. 1972.
- [7] L. C. Oldfield, J. P. Ide, and E. J. Griffin, "A multistate reflectometer," *IEEE Trans. Instrum. Meas.*, vol. IM-34, no. 2, pp. 198–201, Jun. 1985.
- [8] J. R. Juroshek and C. A. Hoer, "A technique for extending the dynamic range of the dual six-port network analyzer," *IEEE Trans. Microw. Theory Tech.*, vol. MTT-33, no. 6, pp. 453–459, Jun. 1985.
- [9] J. J. Yao and S. P. Yeo, "Six-port reflectometer based on modified hybrid couplers," *IEEE Trans. Microw. Theory Tech.*, vol. 56, no. 2, pp. 493–498, Feb. 2008.
- [10] G. F. Engen, "Calibrating the six-port reflectometer by means of sliding terminations," *IEEE Trans. Microw. Theory Tech.*, vol. MTT-26, no. 12, pp. 951–957, Dec. 1978.

- [11] K. Hoffmann and Z. Skvor, "A novel vector network analyzer," *IEEE Trans. Microw. Theory Tech.*, vol. 46, no. 12, pp. 2520–2523, Dec. 1998.
- [12] G. F. Engen, "A (historical) review of the six-port measurement technique," *IEEE Trans. Microw. Theory Tech.*, vol. 45, no. 12, pp. 2414–2417, Dec. 1997.
- [13] S. Ulker and R. M. Weikle, "A millimeter-wave six-port reflectometer based on the sample-transmission line architecture," *IEEE Microw. Wireless Compon. Lett.*, vol. 11, no. 8, pp. 340–342, Aug. 2001.
- [14] D. Rytting, "An analysis of vector measurement accuracy enhancement techniques," in *Proc. Hewlett-Packard RF Microw. Symp. Exhib.*, Mar. 1982, pp. 16–20.
- [15] E. Bergeault, B. Huyart, G. Geneves, and L. Jallet, "Characterization of diode detectors used in six-port reflectometers," *IEEE Trans. Instrum. Meas.*, vol. 40, no. 6, pp. 1041–1043, Dec. 1991.
- [16] Agilent Technologies, Inc., *Agilent 8510C Network Analyzer*, Data Sheet. [Online]. Available: <http://cp.literature.agilent.com/litweb/pdf/5091-8484E.pdf>



**Mohamed A. Abou-Khousa** (S'02) was born in Al-Ain, United Arab Emirates, in 1980. He received the B.S. degree (*magna cum laude*) in electrical engineering from the American University of Sharjah, Sharjah, United Arab Emirates, in 2003, the M.S. degree in electrical engineering from Concordia University, Montreal, QC, Canada, in 2004, and the Ph.D. degree in electrical engineering from Missouri University of Science and Technology (Missouri S&T), Rolla, in 2009.

He is currently a Postdoctoral Fellow with the Applied Microwave Nondestructive Testing Laboratory (*amntl*), Electrical and Computer Engineering Department, Missouri S&T. His current research interests include millimeter-wave and microwave instrumentation, numerical electromagnetic analysis, modulated antennas, RF design, and wideband wireless communication systems.

Dr. Abou-Khousa frequently serves as a Reviewer for various IEEE technical publications.



**Mark A. Baumgartner** was born in Atchison, KS, in 1988. He received the A.S. degree from Northwest Missouri State University, Maryville, in 2006. He is currently working toward the B.S. degree in electrical engineering and computer science with Missouri University of Science and Technology (Missouri S&T), Rolla.

He is currently an Undergraduate Laboratory Assistant with the Applied Microwave Nondestructive Testing Laboratory (*amntl*), Electrical and Computer Engineering Department, Missouri S&T. His areas of

interest include measurement and instrumentation, RF design, FPGA implementations, measurement automation, and imaging techniques.



**Sergey Kharkovsky** (M'01–SM'03) received the M.S. degree in electronics engineering from Kharkov National University of Radioelectronics, Kharkov, Ukraine, in 1975, the Ph.D. degree in radiophysics from Kharkov National University, Kharkov, in 1985, and the D.Sc. degree in radiophysics from the National Academy of Sciences of Ukraine (NASU), Kharkov, in 1994.

He is currently a Research Associate Professor with the Applied Microwave Nondestructive Testing Laboratory (*amntl*), Electrical and Computer Engineering Department, Missouri University of Science and Technology (Missouri S&T; formerly the University of Missouri-Rolla), Rolla. Prior to joining Missouri S&T in March 2003, he was a Member of Research Staff with the Institute of Radiophysics and Electronics, NASU (IRE NASU), from 1975 to 1998 and was a Professor with the Electrical and Electronics Engineering Department, Cukurova University, Adana, Turkey, from December 1998 to February 2003. He was a Visiting Associate Professor with the Electrical and Computer Engineering Department, Missouri S&T, from March 2003 to February 2006. His research area in IRE NASU was the investigation and development of new millimeter-wave techniques, including dielectric resonators with whispering gallery modes, solid-state oscillators, and their application for material characterization. His current research interest is nondestructive evaluation of composite structures using microwaves and millimeter waves.

Dr. Kharkovsky is an Associate Editor for the IEEE TRANSACTIONS ON INSTRUMENTATION AND MEASUREMENT.



**Reza Zoughi** (S'85–M'86–SM'93–F'06) received the B.S., M.S., and Ph.D. degrees in electrical engineering (radar remote sensing, radar systems, and microwaves) from the University of Kansas, Lawrence.

From 1981 to 1987, he was with the Radar Systems and Remote Sensing Laboratory (RSL), University of Kansas. From 1987 to January 2001, he was with the Department of Electrical and Computer Engineering, Colorado State University (CSU), Fort Collins, where he was a Professor and where he established the Applied Microwave Nondestructive Testing Laboratory (*amntl*). He held the position of the Business Challenge Endowed Professor of Electrical and Computer Engineering from 1995 to 1997 while at CSU. He is currently the Schlumberger Endowed Professor of Electrical and Computer Engineering with Missouri University of Science and Technology (Missouri S&T; formerly the University of Missouri-Rolla), Rolla. He is the author of a textbook entitled *Microwave Nondestructive Testing and Evaluation Principles* (Kluwer Academic Publishers, 2000) and the coauthor (with A. Bahr and N. Qaddoumi) of a chapter on microwave techniques in an undergraduate introductory textbook entitled *Nondestructive Evaluation: Theory, Techniques, and Applications* (edited by P. J. Shull; Marcel and Dekker, Inc., 2002). He is a coauthor of more than 95 journal papers, 229 conference proceedings and presentations, and 81 technical reports. He is the holder of eight patents, all in the field of microwave nondestructive testing and evaluation.

Dr. Zoughi is a Fellow of the American Society for Nondestructive Testing. He is the Editor-in-Chief of the IEEE TRANSACTIONS ON INSTRUMENTATION AND MEASUREMENT. He was the recipient of numerous teaching awards both at CSU and Missouri S&T.